

Optical Engineering

OpticalEngineering.SPIEDigitalLibrary.org

Real-time fiber Bragg grating measurement system using temperature-controlled Fourier domain mode locking laser

Tatsuya Yamaguchi
Yukitaka Shinoda

SPIE.

Tatsuya Yamaguchi, Yukitaka Shinoda, "Real-time fiber Bragg grating measurement system using temperature-controlled Fourier domain mode locking laser," *Opt. Eng.* **56**(6), 066112 (2017), doi: 10.1117/1.OE.56.6.066112.

Real-time fiber Bragg grating measurement system using temperature-controlled Fourier domain mode locking laser

Tatsuya Yamaguchi^{a,*} and Yukitaka Shinoda^b

^aNihon University, Graduate School of Science and Technology, Electrical Engineering, Chiyodaku Kanda, Surugadai, Tokyo, Japan

^bNihon University, College of Science and Technology, Electrical Engineering, Chiyodaku Kanda, Surugadai, Tokyo, Japan

Abstract. We constructed a temperature-controlled Fourier domain mode locking (TC-FDML) laser capable of high-speed wavelength sweeping and developed a real-time fiber Bragg grating (FBG) measurement system. The TC-FDML laser can perform high-speed wavelength sweeping at a sweep frequency of 50.7 kHz with a scan range of ~60 nm in the 1.55- μm band. This system uses a data acquisition system mounting an analog/digital converter and field programmable gate array that enables real-time FBG measurement at a sampling frequency of 250 MHz. Using bidirectional wavelength sweeping by the TC-FDML laser, the system has a measurement time resolution of 9.9 μs . We show that the developed system can measure high-speed vibrations of several kHz and perform simultaneous and continuous measurements of multiple FBGs for a period of one hour. © The Authors. Published by SPIE under a Creative Commons Attribution 3.0 Unported License. Distribution or reproduction of this work in whole or in part requires full attribution of the original publication, including its DOI. [DOI: [10.1117/1.OE.56.6.066112](https://doi.org/10.1117/1.OE.56.6.066112)]

Keywords: fiber Bragg grating; temperature-controlled Fourier domain mode locking laser; real-time measurement; vibration measurement; wavelength-swept laser; field programmable gate array.

Paper 170374 received Mar. 16, 2017; accepted for publication Jun. 5, 2017; published online Jun. 21, 2017.

1 Introduction

Compared with electrical sensors, optical fiber sensors have the advantage of being explosion-proof, highly corrosion resistant, and robust to electromagnetic induction and electromagnetic noise. In addition, the use of light negates the need for a power supply in the sensor section making it possible to embed optical fiber sensors in structures.^{1,2} Because of these features, the use of optical fiber sensors for structural health and deterioration monitoring in large-scale buildings, bridges, etc., has been attracting attention.³ A fiber Bragg grating (FBG) in an optical fiber sensor forms a diffraction grating within the core of the optical fiber so that only light of the Bragg wavelength is reflected. If strain is applied in the longitudinal direction of the optical fiber, the wavelength reflected by the FBG will shift. The amount of this shift is proportional to the applied strain, which is the principle of strain measurement using an FBG. At the same time, an FBG transmits light other than the reflected wavelength, which makes it possible to multiplex FBGs having different Bragg wavelengths.¹⁻³

A variety of optical systems³⁻¹¹ have been proposed for measuring the reflected wavelength of an FBG, such as interferometers, spectroscopic systems, and wavelength-swept systems. A wavelength-swept system, in particular, can be constructed using only a wavelength-swept laser and a detector. This type of system obtains information on the FBG reflected wavelength by sweeping the lasing wavelength of the laser and applying time-resolved measurement to the FBG reflected light. The use of a high-speed wavelength-swept laser in this way improves temporal resolution and enables high-speed measurements. The development of such high-speed measurement systems should lead to a wide

range of applications,¹²⁻¹⁴ such as vibration measurement in the ultrasonic range and nondestructive inspection, using the acoustic-emission method.

On the other hand, a wavelength-swept laser using a wavelength filter suffers from a noticeable drop in laser optical output at sweep frequencies in excess of several tens of kHz.^{15,16} In response to this problem, Fourier domain mode locking (FDML) has been proposed as a new control method that enables high-speed sweeping at frequencies above several tens of kHz.¹⁷ As a result, there has been much research on using FDML-based wavelength-swept lasers (FDML laser) as a light source in optical coherence tomography in the 1.3- μm band.^{17,18} Trials have also been conducted on the use of FDML lasers for FBG measurement, and the measurement of FBG reflected light at laser sweep frequencies of several tens of kHz has been reported.¹⁹⁻²¹ A system combining the FDML laser and field programmable gate array (FPGA) has been tried.²² However, demonstration of long-time continuous measurement using the FDML laser has not been reported. Therefore, to ensure the temporal stability of the sweep wavelength of the FDML laser, we constructed a temperature-controlled FDML (TC-FDML) laser.²³ The TC-FDML laser uses the thermal chambers to control the temperature of the fiber Fabry-Perot tunable filter (FFP-TF) and the fiber of 2 km. The TC-FDML laser can perform high-speed wavelength sweeping of ~60 nm at a sweep frequency of 50.7 kHz. Conventionally, only the forward scan of the sinusoidal sweeping was used to the wavelength calculation method. Accordingly, we realized wavelength calculation using both forward scan and backward scan bidirectionally. Therefore, a time resolution of 9.9 μs corresponding to twice the sweep frequency can be obtained. When the laser is swept at a high speed, the propagation time (delay time) of the distance to the installed FBG becomes a problem. In other words, there is a problem that the FBG reflected wavelength shifts to the long

*Address all correspondence to: Tatsuya Yamaguchi, E-mail: csta15001@g.nihon-u.ac.jp

wavelength side in forward scan and short wavelength side in backward scan. We solved this problem by calculating and removing delay times using forward scan and backward scan bidirectional sweeping. Then, we developed a real-time FBG measurement system using the TC-FDML laser. This system meets the need for high-speed signal processing in response to the TC-FDML laser and achieves real-time FBG measurement by using a data acquisition (DAQ) system mounting an analog/digital converter (ADC) and FPGA. This system demonstrated that it can perform real-time measurements of multiple FBGs for a period of 1 h by using the TC-FDML laser and digital computation with FPGA.

2 Experimental Equipment

2.1 TC-FDML Laser

The configuration of the TC-FDML laser lasing in the 1.55- μm band is shown in Fig. 1. The optical system of this TC-FDML laser consists of a fiber ring cavity made up of a semiconductor optical amplifier (SOA), two isolators, FFP-TF, a coupler, and a circulator. The temperature-controlled SOA (1117S, Thorlabs) functions as the gain medium of the TC-FDML laser having a center wavelength of 1554.2 nm. Two isolators are inserted on either side of the SOA so that light circulates within the cavity in one direction. The FFP-TF (Lambda Quest) is an optical wavelength filter that passes only light of specific wavelengths. Transparent wavelengths of the FFP-TF can be set as desired by a control signal. This FFP-TF features a center wavelength of 1550 nm, a finesse of 749, and a free spectral range of 119.2 nm. Its drive system consists of an oscillator (OSC) (33612A, Agilent Technologies) and high-output amplifier (AMP) (33502A, Agilent Technologies). The OSC generates a sinusoidal waveform as an FFP-TF drive signal and controls the FFP-TF via the AMP. In contrast to a conventional wavelength-swept laser, this TC-FDML laser inserts several km of fiber within the cavity. This is done to control the time that light circulates within the cavity and to synchronize the circulating light with the sweep frequency of the FFP-TF. The TC-FDML laser that we

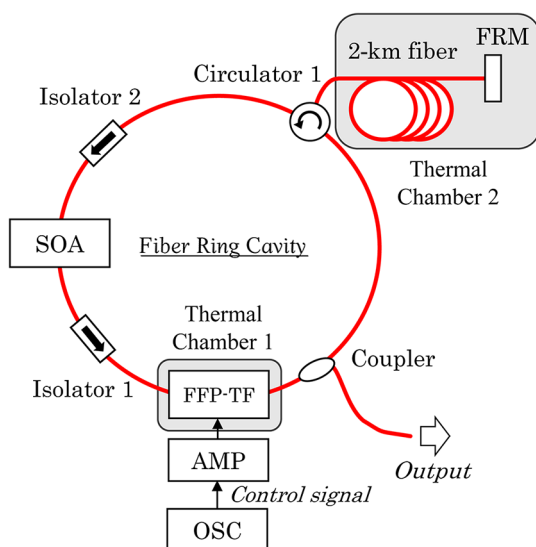


Fig. 1 TC-FDML laser.

constructed uses 2 km of fiber, one end of which connects to a Faraday rotator mirror (FRM). This FRM reflects the light propagating through the fiber making the length of the fiber equivalent to 4 km. The TC-FDML laser, therefore, performs bidirectional wavelength sweeping from short to long wavelengths (forward scan) and from long to short wavelengths (backward scan) at a sweep frequency f_m of 50.7 kHz. In addition, both the FFP-TF and the 2 km of fiber are kept at a temperature of 25°C through the use of thermal chambers (SLC-25A, Mitsubishi Electric Engineering) 1 and 2 using the Peltier system.

2.2 Real-Time FBG Measurement System Using TC-FDML Laser

The configuration of our real-time FBG measurement system using a TC-FDML laser is shown in Fig. 2. This system consists of an optical system and measurement system.

The optical system consists of the TC-FDML laser, a circulator, five FBGs acting as strain sensors, and a detector. The light output from the TC-FDML laser enters the FBGs via the circulator. The Bragg wavelengths λ_{Bk} ($k = 1$ to 5) of FBG $_k$ ($k = 1$ to 5) are 1530, 1540, 1550, 1560, and 1565 nm, each having a reflectivity of $\sim 80\%$ and a half width of ~ 0.2 nm. The light reflected from each FBG enters the detector (P6713, Tektronix) again via the circulator. Detector characteristics consist of a frequency bandwidth of DC 300 MHz and a wavelength bandwidth of 1100 to 1700 nm. The distances L_k ($k = 1$ to 5) of FBG $_k$ ($k = 1$ to 5) from reference point P_R are 7.19, 12.43, 18.01, 23.52, and 29.34 m. Here, the system has been designed so that delay fiber of length ΔL can be inserted between FBG $_1$ and FBG $_2$ with the result that distances L_2 to L_5 are incremented exactly by delay-fiber length ΔL . In addition, reference point P_R serves as the position for measuring the correspondence between the TC-FDML laser wavelength and time as described in Sec. 4.2.

The measurement system consists of a DAQ system (PXIe-1071, National Instruments) and a personal computer (PC). The DAQ inputs a detector signal, a trigger signal synchronized with the OSC control signal, and a 10-MHz reference clock signal to perform frequency synchronization. This DAQ mounts a digitizer integrating an ADC, FPGA, and a transmitter. The digitizer (PXIe-5170R, National Instruments) has four 14-bit analog input channels and can perform in-line signal processing with a sampling frequency f_s of 250 MHz. The results of signal processing are transferred to the PC via the transmitter (PXIe-8381, National Instruments) having a maximum transfer bandwidth of 3.2 GB/s. A direct memory access system is also used here to speed up data transfer from the DAQ to the PC.

In the experiment, sweep frequency f_m of the TC-FDML laser was driven at 50.7 kHz and the light reflected by each FBG was measured using bidirectional wavelength sweeping. This system can measure the reflected wavelength of each FBG at each half period of the TC-FDML laser's sweep period resulting in a time resolution t_r ($=1/2f_m$) of 9.9 μs .

This system was developed using LabVIEW (National Instruments), a graphical programming language. The monitor screen of this real-time FBG measurement system is shown in Fig. 3. This screen is divided into a control section and display section. The control section is used to check the

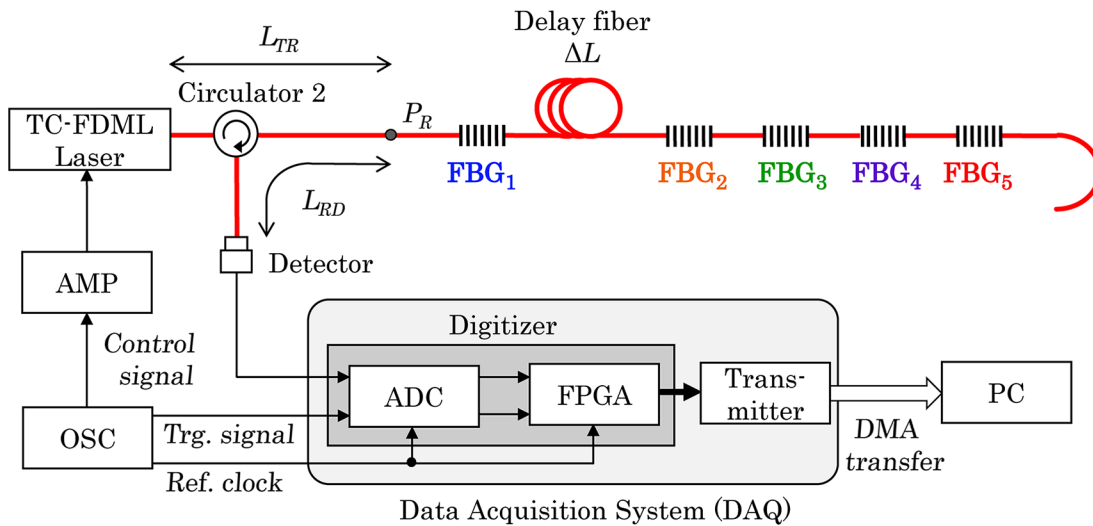


Fig. 2 Real-time FBG measurement system using TC-FDML laser.

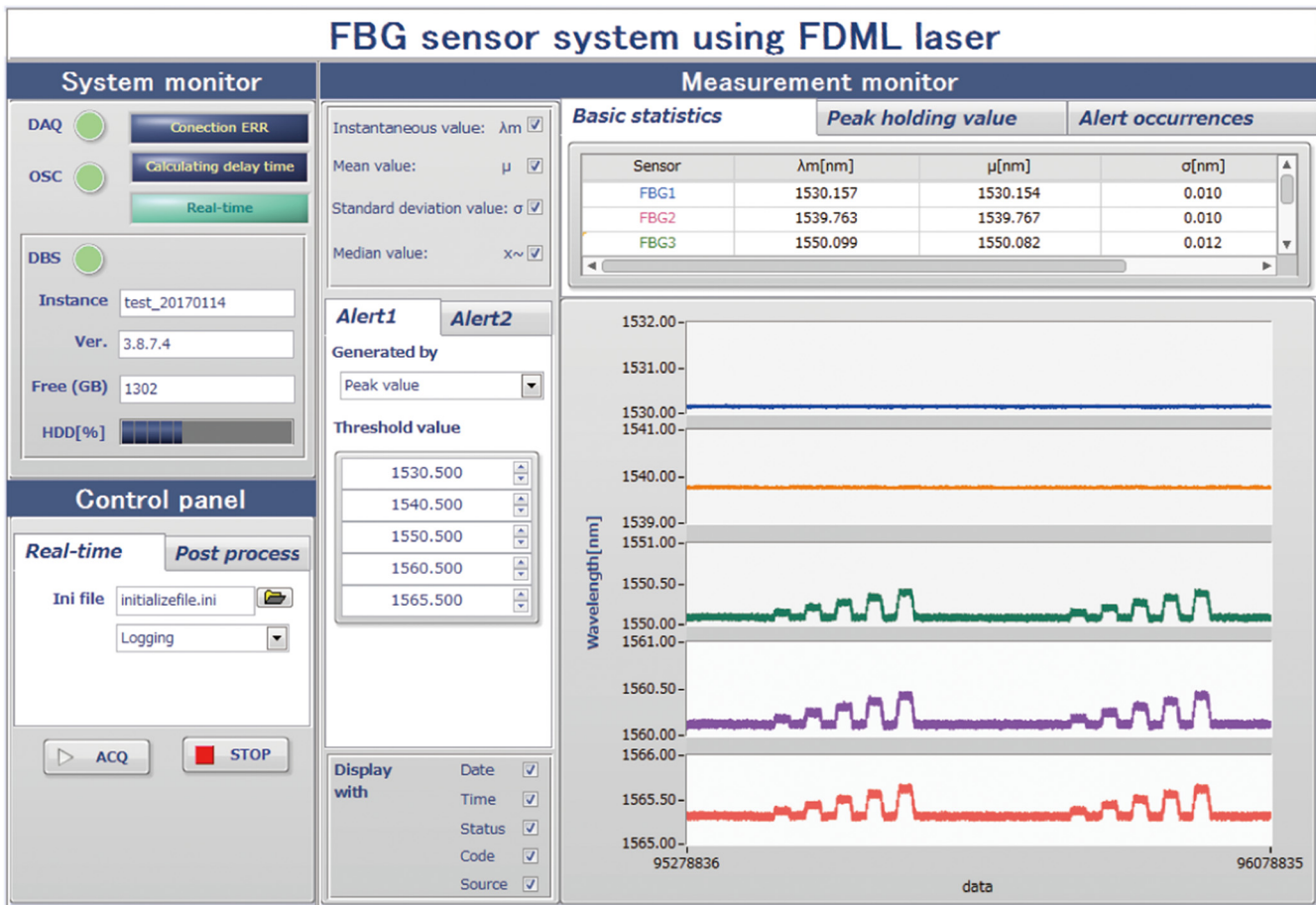


Fig. 3 Monitor screen of real-time FBG measurement system.

operation status of the measurement system consisting of DAQ, OSC, etc., and to make DAQ settings. The display section, meanwhile, provides real-time display of reflected wavelengths from each FBG. These reflected-wavelength measurement data are simultaneously stored in a binary file. To execute multiple tasks with good efficiency, the system internally implements parallel distributed processing,

which enables it to monitor the reflected wavelengths of multiple FBGs in real time. The screenshot in Fig. 3 shows the monitoring of reflected wavelengths during dynamic application of strain. It can be seen from the results shown how the reflected wavelengths of these FBGs respond to strain. In short, this system can perform real-time monitoring of reflected wavelengths from multiple FBGs.

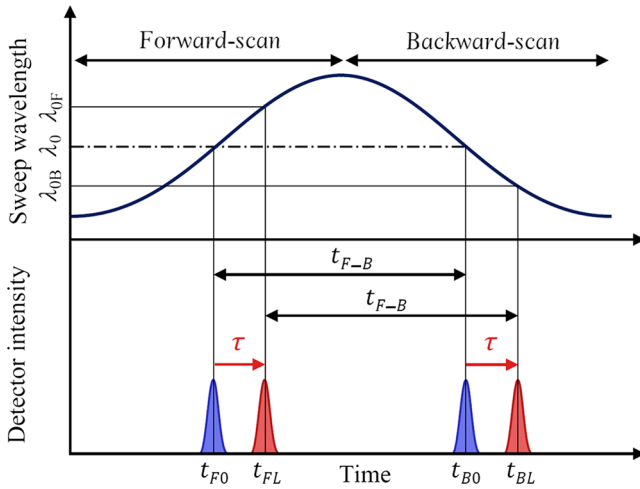


Fig. 4 Concept of FBG measurement by wavelength sweeping method.

3 Measurement Method

The concept of FBG measurement by a wavelength-swept system is shown in Fig. 4. In this method, the laser performs wavelength sweeping using a sinusoidal signal for the control signal. When light from the laser becomes incident on an FBG, a reflection spectrum of that FBG is obtained at the detector. This reflection spectrum shifts according to the Bragg wavelength of the FBG. It is therefore possible to calculate the wavelength from the time of that reflection spectrum. Now, denoting the FBG reflected wavelength as λ_0 , forward-scan and backward-scan sweeping by the laser results in detection of the FBG reflection spectrum at times t_{F0} and t_{B0} , which corresponds to a measurement of wavelength λ_0 . However, if laser sweep frequency is high and optical propagation time cannot be ignored, this measurement will be affected by delay time τ due to fiber length from the measurement system to the FBG. Specifically, the FBG reflection spectrum will instead be detected at times t_{FL} and t_{BL} , which means that the converted wavelength will likewise shift from the original λ_0 to λ_{0F} in the forward scan and λ_{0B} in the backward scan. To solve this problem, it is necessary to take into account delay time associated with fiber length.

3.1 Delay Time Calculation

The signal-processing flow shown in Fig. 5 is used to calculate delay time. To begin with, the detector signal V_D is detected as FBG reflection-spectrum times t_{FL} and t_{BL} by signal processing using the FPGA. Time difference t_{F-B} as shown in Fig. 4 can now be calculated from these two detected reflection-spectrum times. This time difference t_{F-B} changes according to the FBG reflected wavelength, so it can be converted to the original wavelength. In addition, since time difference t_{F-B} can be expressed by Eq. (1), it can be seen that the delay-time terms cancel out, which means that wavelength conversion can be performed without being affected by that delay time

$$t_{F-B} = t_{BL} - t_{FL} = (t_{B0} + \tau) - (t_{F0} + \tau). \quad (1)$$

That is to say, the FBG wavelength λ_0 can be calculated from time difference t_{F-B} . This value of λ_0 can then be

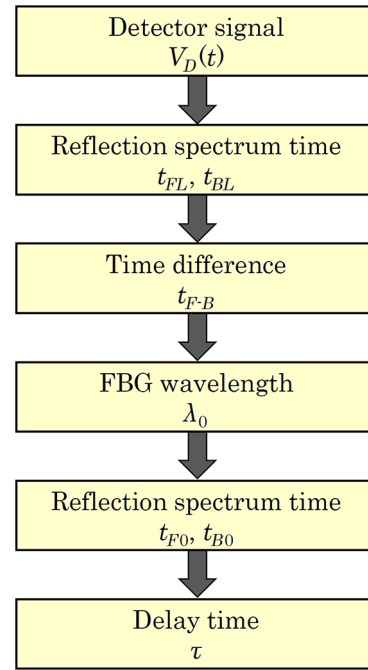


Fig. 5 Calculation flow of delay time τ .

converted to FBG reflection-spectrum times t_{F0} and t_{B0} , which can then be used to calculate delay time τ .

3.2 FBG Reflection-Spectrum Detection Algorithm by FPGA

Signal processing using an FPGA device was introduced to speed up the detection of FBG reflection spectrums. The signal processing flow using an FPGA is shown in Fig. 6. First, the analog/digital conversion of the detector signal is activated by the trigger signal and the resulting digital data are transferred to the FPGA. Next, the FPGA extracts the FBG reflection spectrum from the detector signal V_D by threshold processing. It then holds data number N_0 corresponding to the position of peak amplitude in the extracted reflection spectrum and the two data items on either side of that peak point for a total of five data items. The FPGA then uses this held data to calculate centroid peak N_{cp} by the centroid peak detection method of Eq. (2). It also calculates reflection spectrum time t_{cp} by Eq. (3) using centroid position N_{cp}

$$N_{cp} = \frac{\sum_{i=N_0-M_m}^{N_0+M_m} V_D(i) \times i}{\sum_{i=N_0-M_m}^{N_0+M_m} V_D(i)}, \quad (2)$$

$$t_{cp} = N_{cp} \times t_s, \quad (3)$$

where M_m is the number of data items before and after the peak position, which is here set to $M_m = 2$. In addition, $t_s (=1/f_s)$ is the sampling time interval, which is 4 ns in this study.

We point out here that if only data number N_0 were to be used in peak position detection, a problem would arise in that the resolution of peak position detection would be dependent on sampling frequency. This system therefore enhances resolution in peak position detection by using the centroid peak

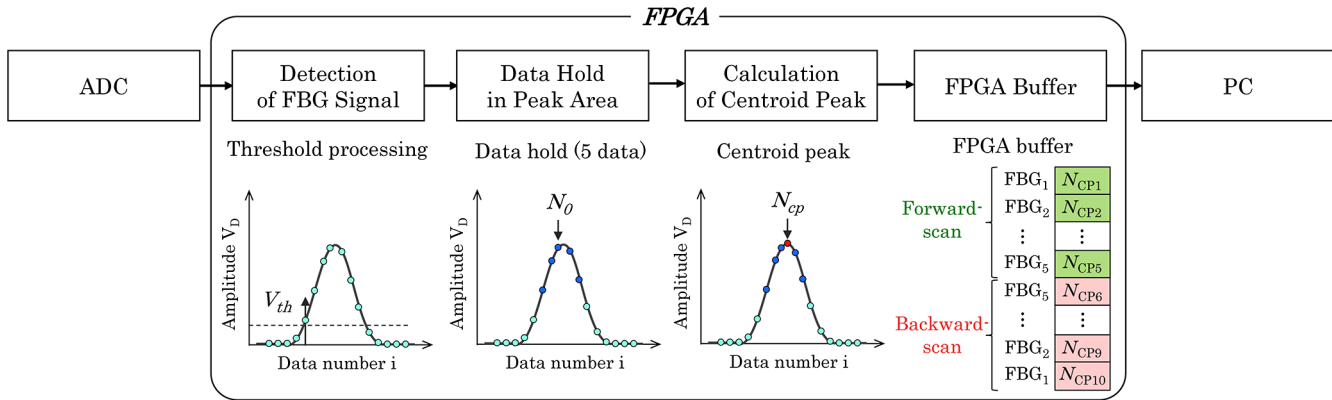


Fig. 6 Flow of FPGA signal processing.

detection method. Moreover, to perform real-time measurements, this sequence of processes must be carried out for each FBG reflection spectrum in forward and backward scanning and output within the TC-FDML laser's sweep period. The FPGA therefore incorporates parallel processing using pipeline processing to achieve high-speed signal processing. The results of calculating centroid peak N_{cp} of each FBG reflection spectrum by FPGA are successively input into a first-in first-out buffer within the FPGA and transferred to the PC.

3.3 Real-Time Calculation of Reflected Wavelengths

To achieve real-time measurement of FBG reflected wavelengths, centroid peaks N_{cp} of the FBG reflection spectrums obtained by FPGA signal processing are first transferred to the PC to calculate times t_{FL} and t_{BL} of those reflection spectrums using Eq. (3). Next, using delay time τ calculated as described in Sec. 3.1, this value of τ is subtracted from times t_{FL} and t_{BL} of the reflection spectrums. This removes the effect of delay time and calculates times t_{F0} and t_{B0} of the FBG reflection spectrums. Reflected wavelength λ_0 can then be calculated from times t_{F0} and t_{B0} determined in the above way. The calculated reflected wavelengths of each FBG are simultaneously displayed on the monitor screen and the data are saved. Thus, by using delay time τ calculated beforehand and correcting the detected time of each forward-scan and backward-scan reflection spectrum, this method is able to calculate a reflected wavelength in half the sweep period.

4 Experimental Results

4.1 Measurement of TC-FDML Laser Characteristics, and FBG Reflection Spectrums

To begin with, we measured the wavelength-swept output of the TC-FDML laser that we constructed using an optical spectrum analyzer (AQ6317B, ANDO), setting the number of measurements to be averaged to 100.

The results of measuring the TC-FDML laser swept band are shown in Fig. 7. The TC-FDML laser is driven at a sweep frequency f_m of 50.7 kHz. It can be seen from these results that the laser has a scan range of ~ 60 nm from 1520 to 1580 nm. Measurements with a power meter (PM100USB, Thorlabs) revealed an optical output of 2.02 mW.

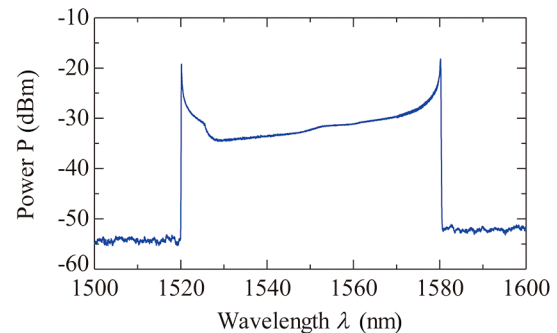


Fig. 7 Output spectrum of TC-FDML laser.

Next, we fed this swept output from the TC-FDML laser into the FBG measurement system and measured the reflection spectrum of multiple FBGs. Sweep frequency f_m of the TC-FDML laser was set to 50.7 kHz and sampling frequency f_s of the DAQ to 250 MHz.

The results of measuring the reflection spectrum of FBGs using the TC-FDML laser are shown in Fig. 8. First, Fig. 8(I) shows measurement results for no delay fiber inserted between FBG_1 and FBG_2 ($\Delta L = 0$ m). Here, Fig. 8(I-a) shows the control signal of the TC-FDML laser oscillator and Fig. 8(I-b) shows the FBG reflection spectrum for the forward and backward scans. Times t_{FL} and t_{BL} in the forward and backward scans can be measured for each of the five installed gratings FBG_k ($k = 1$ to 5) from its reflected signals that include delay time corresponding to distance L_k of that FBG. The numerals in the figure indicate the number k of each FBG. It can be seen from these results that the use of bidirectional wavelength sweeping by the TC-FDML laser enables detection of FBG reflected signals every $9.9 \mu s$ corresponding to half the sweep period. Next, Fig. 8(II) shows measurement results for delay fiber inserted between FBG_1 and FBG_2 ($\Delta L = 30$ m). It can be seen that the reflected signals of gratings FBG_2 to FBG_5 are shifted compared with the above results due to the effect of the delay fiber. We therefore investigated the relationship between distance L_k ($k = 1$ to 5) from reference point P_R to FBG_k and the time of the FBG reflected signal.

The time of the reflected signal for each FBG while varying distance L_k using delay fiber length ΔL is shown in Fig. 9. First, Fig. 9(a) shows the results of measuring time t_{FL} of the reflected signal for each of the five FBGs in the forward scan.

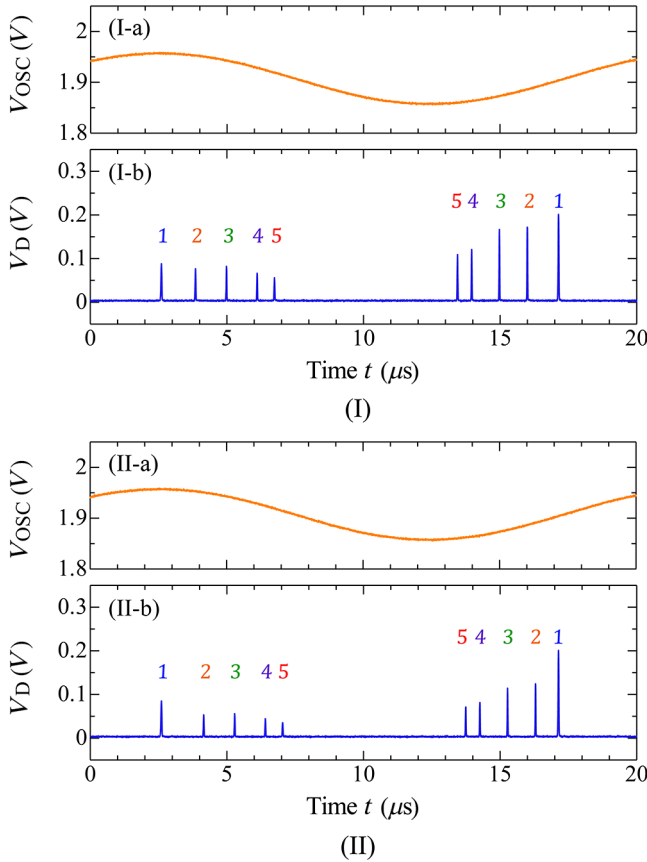


Fig. 8 Reflection spectrum of FBGs: (I) $\Delta L = 0$ m, (I-a) laser control signal, (I-b) FBG reflection signals, (II) $\Delta L = 30$ m, (II-a) laser control signal, and (II-b) FBG reflection signals.

These results show that lengthening delay fiber length ΔL increases the time of the reflected signal for gratings FBG₂ to FBG₅. In addition, the slope of the line of best-fit by the method of least squares turns out to be 9.8 ns/m for gratings FBG₂ to FBG₅. Here, delay time τ_k ($k = 1$ to 5) due to distance L_k ($k = 1$ to 5) from reference point P_R to FBG _{k} ($k = 1$ to 5) is given as

$$\tau_k = \frac{2nL_k}{c}, \quad (4)$$

where c is the speed of light and n is the refractive index of the optical fiber.

Given a fiber length of 1 m, delay time τ from Eq. (4) is 9.8 ns, which agrees with the slope of the best-fit line calculated from the results of Fig. 9(a). We therefore attempted to remove delay time using the delay-time calculation method described in Sec. 3.1.

Next, Fig. 9(b) shows the results of measuring time $(t_{FL} - \tau_k)$ of the reflected signal when removing delay time τ_k . As shown, time $(t_{FL} - \tau_k)$ is constant indicating no effect of delay-fiber length ΔL . In addition, the effect of distance L_k of each FBG at $\Delta L = 0$ m could likewise be removed enabling the calculation of time t_{F0} . These results show that this technique can remove the delay time associated with distance L_k from reference point P_R to FBG _{k} in Fig. 2 and can calculate time t_{F0} of the reflected signal. The same kind of processing can be applied to the backward scan to calculate time t_{B0} of the reflected signal.

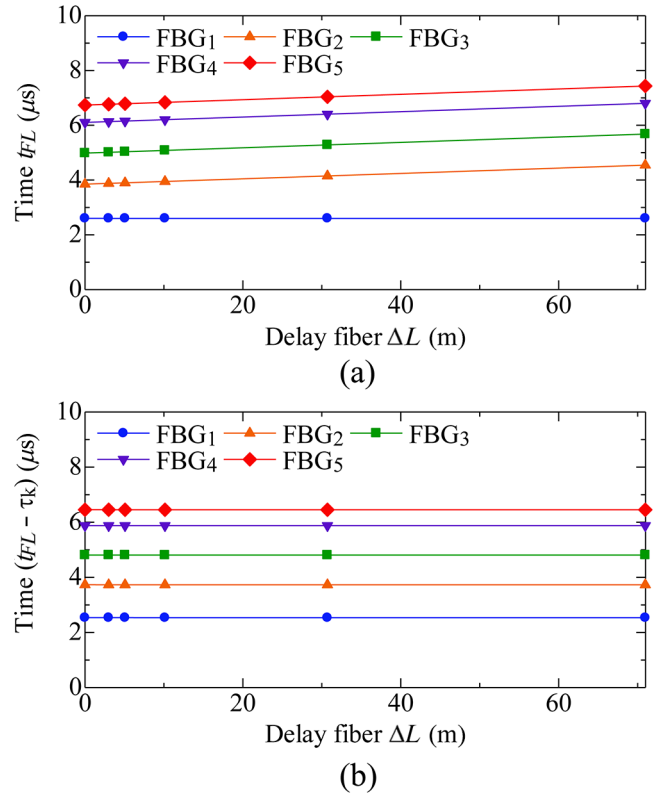


Fig. 9 Result of reflection spectrum by delay fiber: (a) results when affected by delay time and (b) results when removing delay time.

4.2 Measurement of TC-FDML-Laser Swept Wavelengths

Measurement of FBG reflected wavelengths requires prior measurement of the relationship between the wavelengths generated by the TC-FDML laser and times t_{F0} and t_{B0} measured by the FBG measurement system.

We therefore inputted the swept wavelengths of the TC-FDML laser into an optical tunable filter (OTF) (FFM-C, Axsun Technologies) and detected the transmission spectrum at that time by the detector of the FBG measurement system (Fig. 10). Transparent wavelengths of the OTF can be set as desired by a digital/analog converter (PCIe-6361, National Instruments). We also measured time t_c of that transmission spectrum using the DAQ and simultaneously measured wavelength λ_{WM} of the transmission spectrum using a spectroscopic wavelength monitor (WM) (FB200, ANDO). The wavelength resolution and measurement wavelength band of this WM were 1 pm and 1527 to 1567 nm, respectively. In this experiment, we set the fiber length L_R ($=L_{TR} + L_{RD}$) from the TC-FDML laser to the detector via the OTF to match the propagation time of light reflected from reference point P_R in the FBG measurement system of Fig. 2. In Fig. 2, the fiber length L_{TR} is the length from the TC-FDML laser to the reference point P_R , and the fiber length L_{RD} is the length from the reference point P_R to the detector. In this way, measured time t_c would correspond to times t_{F0} and t_{B0} of the reflection spectrum in the FBG measurement system.

The results of measuring the TC-FDML laser wavelength and of approximating the polynomial of that data are shown

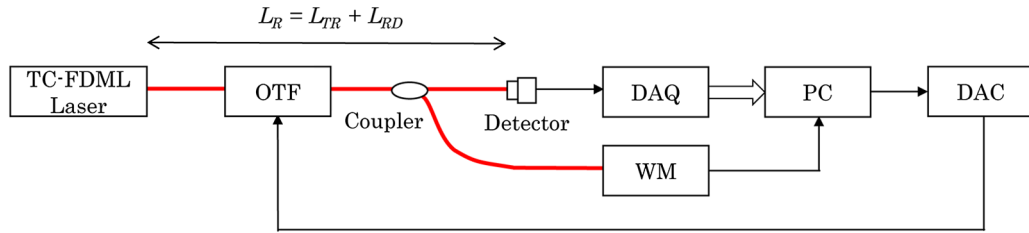


Fig. 10 Setup for measuring TC-FDML-laser swept wavelengths.

in Fig. 11. As shown, the lasing wavelengths in both the forward scan and backward scan of the TC-FDML laser could be measured indicating a sinusoidal sweep with a sweep frequency of 50.7 kHz. This means that wavelength can be converted from time using this polynomial approximation. In this system, the reflected wavelength in both the forward scan and backward is converted from time using this polynomial curve after calculating times t_{F0} and t_{B0} of the FBG reflection spectrum.

4.3 Static Strain Measurement

To apply static strain, a fixed stage and a movable stage (SGSP-26-100, SIGMA KOKI) were affixed to opposite ends of the fiber that included the FBG_4 grating. The interval L_{stage} between these two stages was 1 m. Shifting the movable stage by ΔX_{FBG4} (μm) would apply a strain of $\Delta \epsilon_{FBG4}$ ($\mu \epsilon$) ($=\Delta X_{FBG4}/L_{stage}$). The amount of stage movement ΔX_{FBG4} was increased in 100 μm increments, and measurements were performed using the developed system.

The results of FBG_4 reflected wavelengths due to strain when affected by delay time are shown in Fig. 12. First, Fig. 12(a) shows the results with no delay fiber inserted ($\Delta L = 0$ m). As shown, the values of the reflected wavelengths in both the forward scan and backward scan shifted to the side of longer wavelengths as strain was applied. Here, if we examine the reflected wavelengths at $\Delta X_{FBG4} = 0 \mu m$, we have 1562.20 and 1558.06 nm for the forward scan and backward scan, respectively. This is because the delay time caused by the distance from reference point P_R to FBG_4 has the effect of shifting the reflected wavelength in the forward scan to a longer wavelength and that in the backward scan to a shorter wavelength. Now, Fig. 12(b) shows the results with delay fiber inserted ($\Delta L = 30$ m). In this case, the reflected wavelengths at $\Delta X_{FBG4} = 0 \mu m$ were 1564.73

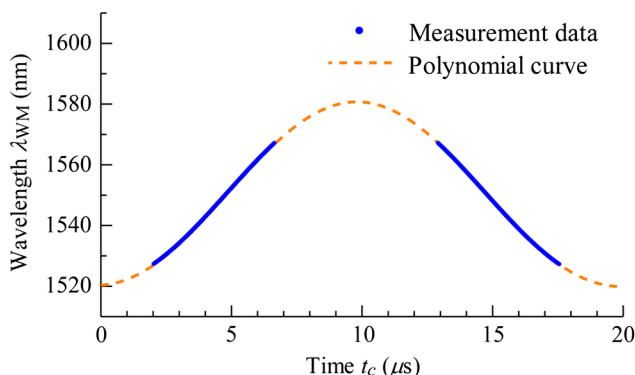


Fig. 11 Sweep wavelength of TC-FDML laser.

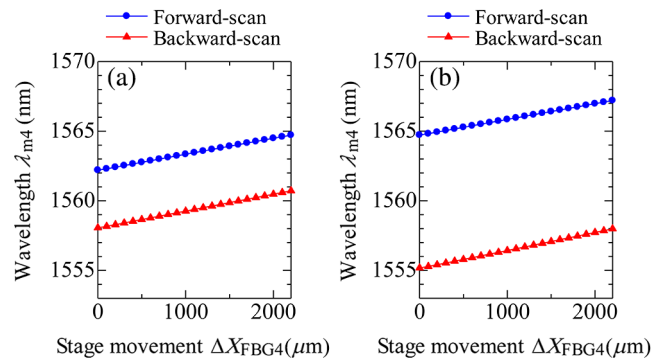


Fig. 12 Results of reflected wavelengths due to strain when affected by delay time: (a) $\Delta L = 0$ m and (b) $\Delta L = 30$ m.

and 1555.18 nm in the forward scan and backward scan, respectively, which shows that the amount of shift increases when inserting delay fiber. The above results underscore the necessity of taking delay time into account when measuring FBGs by a wavelength-swept system. Next, the results of FBG_4 reflected wavelengths due to strain when removing delay time are shown in Fig. 13. On examining the reflected wavelength for $\Delta X_{FBG4} = 0 \mu m$ in Fig. 13(a), we see that the reflected wavelength in both the forward scan and backward scan is 1560.15 nm, which indicates that the effect of delay time caused by the distance from P_R to FBG_4 could be removed. The effect of delay time could likewise be removed for the case of inserting delay fiber as shown in Fig. 13(b). The slope of the best-fit line for these results as calculated by the method of least squares came to $\sim 1.2 \times 10^{-3}$ nm/ μm for both the forward scan and backward scan. These results show that the system can remove the effect of delay time

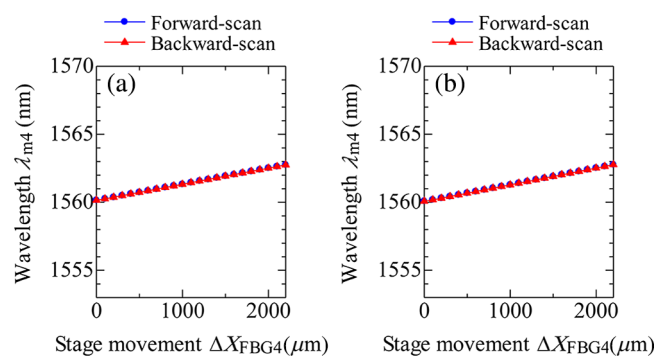


Fig. 13 Results of reflected wavelengths due to strain when removing delay time: (a) $\Delta L = 0$ m and (b) $\Delta L = 30$ m.

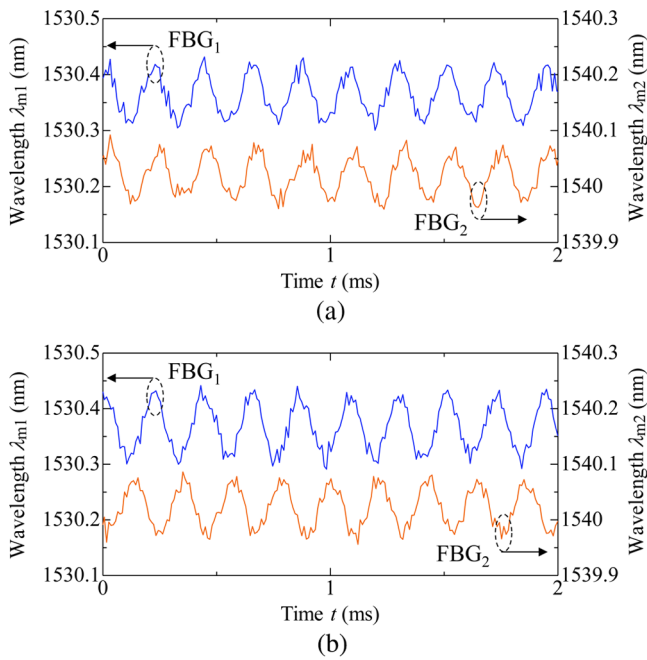


Fig. 14 Time response of reflection wavelength by high-speed vibration: (a) $\phi_1 = \phi_2$ and (b) $\phi_2 - \phi_1 = \pi$.

and calculate reflected wavelengths using forward-scan and backward-scan bidirectional sweeping.

4.4 High-Speed Vibration Measurement

We applied vibration using two piezoelectric vibrators to test whether this system is capable of measuring high-speed vibration. In this experiment, we affixed piezoelectric vibrators 1 and 2 to FBG₁ and FBG₂, respectively, and set vibration frequency f_v to 4.65 kHz.

The time-response waveforms of reflected wavelengths from FBG₁ and FBG₂ when simultaneously driving the two piezoelectric vibrators are shown in Fig. 14. First, Fig. 14(a) shows results for in-phase ($\phi_1 = \phi_2$) application of voltage from piezoelectric vibrators 1 and 2. As shown, the reflected wavelengths of FBG₁ and FBG₂ were found to oscillate in a sinusoidal manner at the piezoelectric-vibrator vibration frequency of 4.65 kHz with a change in reflected wavelength of ~ 0.1 nm. This system can measure reflected

wavelengths every $9.9 \mu s$ by using bidirectional wavelength sweeping by the TC-FDML laser. Next, Fig. 14(b) shows results when applying voltage from piezoelectric vibrators 1 and 2 with a phase difference ($\phi_2 - \phi_1$) of π . These results show that the phase relationship between these two high-speed vibration waveforms could be measured. They also demonstrate that this system could measure high-speed vibrations of several kHz and measure the phase relationship between the vibration waveforms of two FBGs.

4.5 Real-Time Measurement of Reflected Wavelengths

Next, we performed real-time measurement of reflected wavelengths to test whether this system is capable of high-speed and long-term measurements. Similar to the measurement of static strain described in Sec. 4.3, we affixed the same type of movable stages to FBG₃ and FBG₅ and applied instantaneous strain every 10 min. This strain was produced by driving the movable stage with a series of pulses changing the amount of movement in the order of 50, 100, 150, 200, and 250 μm at intervals of 400 ms.

The results of real-time measurement of reflected wavelengths for a period of 1 h are shown in Fig. 15. Specifically, Figs. 15(a), 15(b), and 15(c) show results for the reflected wavelengths of FBG₁, FBG₃, and FBG₅, respectively. The results of Figs. 15(b) and 15(c), in particular, show that the system could measure this instantaneous strain applied every 10 min. Here, the standard deviation of reflected-wavelength

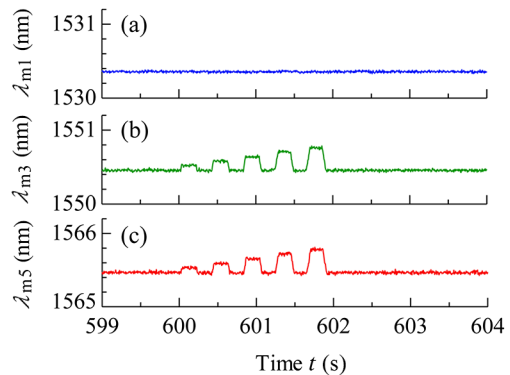


Fig. 16 Enlarged view of Fig. 15 at 10 min: (a) FBG₁, (b) FBG₃, (c) FBG₅.

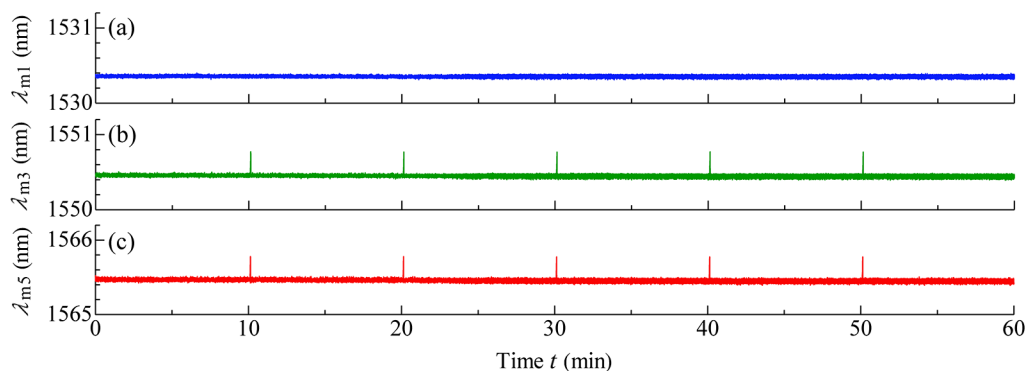


Fig. 15 Real-time measurement of reflection wavelengths: (a) FBG₁, (b) FBG₃, (c) FBG₅.

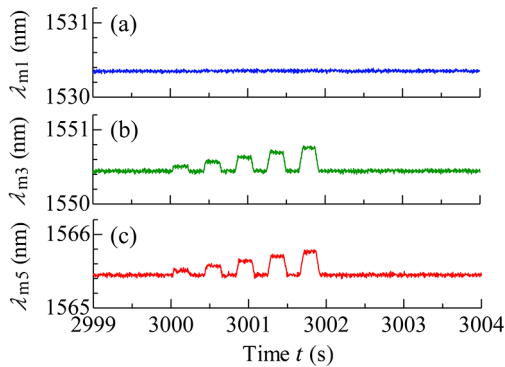


Fig. 17 Enlarged view of Fig. 15 at 50 min: (a) FBG₁, (b) FBG₃, (c) FBG₅.

values when not applying strain was under 1.3×10^{-2} nm in all cases. An enlarged view of the results of Fig. 15 at $t = 10$ min is shown in Fig. 16. These results show that the system could measure the change in the reflected wavelengths of FBG₃ and FBG₅ when applying instantaneous strain. This change in reflected wavelengths due to strain generated by movable-stage shifts of 50, 100, 150, 200, and $250 \mu\text{m}$ came to $\sim 6 \times 10^{-2}$, 12×10^{-2} , 18×10^{-2} , 24×10^{-2} , and 30×10^{-2} nm, respectively. Next, an enlarged view of the results of Fig. 15 at $t = 50$ min is shown in Fig. 17. These results show that the system could measure the same change in reflected wavelengths as those in Fig. 16 even after 50 min of beginning measurements. The above results show that the developed system can handle the measurement of reflected wavelengths over a 1-h period, that it supports high-speed and long-term measurements, and that it can simultaneously monitor the reflected wavelengths of multiple FBGs.

5 Conclusion

The achievements and findings of this study are summarized below.

1. To ensure temporal stability of sweep wavelength of the FDML laser, we constructed a TC-FDML laser lasing in the $1.55\text{-}\mu\text{m}$ band. This TC-FDML laser can perform forward-scan and backward-scan bidirectional wavelength sweeping with a sweep frequency of 50.7 kHz and a scan range of ~ 60 nm.
2. A real-time FBG measurement system using this TC-FDML laser incorporates a DAQ system mounting an ADC and FPGA. This configuration enables signal acquisition with a sampling frequency of 250 MHz and real-time FBG measurement.
3. This system incorporates delay-time calculation enabling measurement of reflected wavelengths that removes the delay time associated with signal propagation along the fiber. As a result, the system achieves a measurement time resolution of half the sweep period, or $9.9 \mu\text{s}$, by using bidirectional wavelength sweeping in the TC-FDML laser.
4. It was shown by experiment that the developed system could simultaneously measure multiple FBG reflected wavelengths, that it could measure

high-speed vibrations of several kHz, and that it could perform these measurements continuously for a period of 1 h.

Future work is to make it possible to measure this system for a longer time. In this system, the amount of data for 1 h reaches ~ 15 GB. Therefore, to measure a longer time, it is necessary to build it using a database that can store and manage enormous amounts of data.²⁴ We plan to extend this system so that it can be measured for a long time.

References

1. A. Othonos and K. Kalli, *Fiber Bragg Grating*, Artech House, London (1999).
2. A. D. Kersey et al., "Fiber grating sensors," *J. Lightwave Technol.* **15**(8), 1442–1463 (1997).
3. J. M. Lopez-Higuera, *Handbook of Optical Fibre Sensing Technology*, Wiley, New York (2002).
4. M. D. Todd, G. A. Johnson, and B. L. Althouse, "A novel Bragg grating sensor interrogation system utilizing a scanning filter, a Mach-Zehnder interferometer and a 3×3 coupler," *Meas. Sci. Technol.* **12**(7), 771–777 (2001).
5. Y. Shinoda et al., "Fundamental experiment of multiple-point measurement for strain by fiber Bragg gratings using optical frequency sweeping," in *Proc. SICE-ICASE Int. Joint Conf.*, pp. 1672–1675 (2006).
6. Z. He, T. Hayashi, and K. Hotate, "High-speed interrogation of multiplexed fiber Bragg grating sensors with similar Bragg wavelength by synthesis of optical coherence function," *Proc. SPIE* **6004**, 600409 (2005).
7. C. G. Askins, M. A. Putnam, and E. J. Friebele, "Instrumentation for interrogating many-element fiber Bragg grating arrays," *Proc. SPIE* **2444**, 257 (1995).
8. S. H. Yun, D. J. Richardson, and B. Y. Kim, "Interrogation of fiber grating sensor arrays with a wavelength-swept fiber laser," *Opt. Lett.* **23**(11), 843–845 (1998).
9. T. Saitoh et al., "Ultra-long-distance fiber Bragg grating sensor system," *IEEE Photonics Technol. Lett.* **19**(20), 1616–1618 (2007).
10. R. Isago and K. Nakamura, "A high reading rate fiber Bragg grating sensor system using a high-speed swept light source based on fiber vibrations," *Meas. Sci. Technol.* **20**(3), 034021 (2009).
11. Y. Nakazaki and S. Yamashita, "Fast and wide tuning range wavelength-swept fiber laser based on dispersion tuning and its application to dynamic FBG sensing," *Opt. Express* **17**(10), 8310–8318 (2009).
12. S. Takeda et al., "Delamination monitoring of laminated composites subjected to low-velocity impact using small-diameter FBG sensors," *Composites Part A Appl. Sci. Manuf.* **36**(7), 903–908 (2005).
13. H. Tsuda et al., "Acoustic emission measurement using a strain-insensitive fiber Bragg grating sensor under varying load conditions," *Opt. Lett.* **34**(19), 2942–2944 (2009).
14. G. Wild and H. Steven, "Acousto-ultrasonic optical fiber sensors: overview and state-of-the-art," *IEEE Sens. J.* **8**(7), 1184–1193 (2008).
15. R. Huber et al., "Amplified, frequency swept lasers for frequency domain reflectometry and OCT imaging: design and scaling principles," *Opt. Express* **13**(9), 3513–3528 (2005).
16. T. Yamaguchi and Y. Shinoda, "Development of fast FBG interrogator with wavelength-swept laser," *Proc. SPIE* **9506**, 95061F (2015).
17. R. Huber, M. Wojtkowski, and J. G. Fujimoto, "Fourier domain mode locking (FDML): a new laser operating regime and applications for optical coherence tomography," *Opt. Express* **14**(8), 3225–3237 (2006).
18. M. Gora et al., "Ultra high-speed swept source OCT imaging of the anterior segment of human eye at 200 kHz with adjustable imaging range," *Opt. Express* **17**(17), 14880 (2009).
19. E. J. Jung et al., "Characterization of FBG sensor interrogation based on a FDML wavelength swept laser," *Opt. Express* **16**(21), 16552 (2008).
20. D. Chen, C. Shu, and S. He, "Multiple fiber Bragg grating interrogation based on a spectrum-limited Fourier domain mode-locking fiber laser," *Opt. Lett.* **33**(13), 1395–1397 (2008).
21. B. C. Lee et al., "Dynamic and static strain fiber Bragg grating sensor interrogation with a $1.3 \mu\text{m}$ Fourier domain mode-locked wavelength-swept laser," *Meas. Sci. Technol.* **21**(9), 094008 (2010).
22. M. A. B. Abdallah et al., "High-speed tunable FDML laser, interfaced to a continuous FPGA acquisition system, for FBG accelerometer interrogation," in *2014 IEEE SENSORS* (2014).
23. T. Yamaguchi and Y. Shinoda, "High-speed vibration measurement by fiber Bragg gratings with Fourier domain mode locking laser," *Proc. SPIE* **10323**, 103232I (2017).

24. T. Yamaguchi and Y. Shinoda, "High-speed and long-time FBG interrogation system using wavelength swept laser," *Proc. SPIE* **9525**, 95252X (2015).

Tatsuya Yamaguchi received his BS and MS degrees in electrical engineering from Nihon University, Tokyo, Japan, in 2013 and 2015, respectively. He is pursuing his PhD at Nihon University. He has focused on optical fiber sensing, real-time measurement, and structural health monitoring. He is a student member of SPIE and IEEE.

Yukitaka Shinoda received his BSc, MSc, and PhD degrees in electrical engineering from Nihon University in 1987, 1989, and 2004, respectively. Since 2012, he has been a professor at the College of Science and Technology, Nihon University. He was a visiting researcher at Virginia Polytechnic Institute and State University (Virginia Tech) from 2009 to 2010. He has focused on laser sensing, digital signal processing, motion analysis, and optical scanning holography. He is a member of SPIE, SICE, JSAP, IEIJ, and IEEE.